Electronic Supplementary Information

Anthracene Derivatives Based Multifunctional Liquid Crystal Materials for Optoelectronic Devices

Yunrui Wang[a], Daqi Fang[a], Tianchen Fu[a], Muhammad Umair Ali[a, b], Yuhao Shi[a], Yaowu He*[a], Zhao Hu[c], Chaoyi Yan[a], Zongwei Mei[a], Hong Meng*[a]

[a] School of Advanced Materials, Peking University Shenzhen Graduate School, Shenzhen, 518055, People's Republic of China. E-mail: menghong@pku.edu.cn; heyw@pku.edu.cn

[b] Department of Materials Science and Engineering, College of Engineering, Peking University, Beijing 100871, People's Republic of China.

[c] Department of Applied Physics, The Hong Kong Polytechnic University, Hong Kong.

Contents

General Information

All chemicals and solvents are analytical reagents purchased from commercial sources. 2-(4-octylphenyl)-4, 4, 5, 5-tetramethyl-1, 3, 2-dioxaborolane (**2a**) 2-(4-octyloxyphenyl)-4, 4, 5, 5-tetramethyl-1, 3, 2-dioxaborolane (**2b**) and 2-Bromoanthracene (**3**) were prepared according to the described procedures in the literature.[1-4] 2-Phenyl-4, 4, 5, 5-tetramethyl-1, 3, 2-dioxaborolane was obtained from a commercial source and used without further purification. ^{1}H NMR and ^{13}C NMR were carried out in $CDCl_3$ solution by a Bruker AVANCE 300 MHz or 500 MHz NMR spectrometer.

A three-electrode system, consisted of a glassy carbon electrode as a working electrode, a Pt wire as the counter electrode and an Ag/Ag^{+} as a reference electrode, was applied to perform the cyclic voltammetry (CV) measurements with 0.1 M Bu_4NPF_6 in CH_2Cl_2 served as the supporting electrolyte. The scanning rate of CV measurements is 0.5 V s^{-1}. UV-*vis* absorption spectra were measured in CH_2Cl_2 solution and thin film by a PerkinElmer Lambda 750 spectrophotometer. Photoluminescence spectra were recorded in degassed CH_2Cl_2 solution and thin film by a Horiba Fluorolog-3 spectrofluorometer. Time-resolved photoluminescence spectra in degassed CH_2Cl_2 solution were also obtained by the Horiba Fluorolog-3. Absolute photoluminescence quantum yields (PLQY) in degassed CH_2Cl_2 solution and thin film were determined using the Horiba Fluorolog-3 combined with an integrating sphere. The TA2950 TGA system was used for thermal gravimetric analysis (TGA) and differential scanning calorimetry (DSC) was performed using a Q1000 apparatus. DSC and TGA thermograms were recorded with the heating or cooling rates of 10 ℃ min^{-1} and nitrogen flow rates of 60 cm^3 min^{-1}. Polarized optical microscope (POM) images of the sample powder inside a cell were observed by a ZEISS Axio Scope.A1 microscope combined with the LTS420 thermal stage. Thin film X-ray diffraction (XRD) was characterized by a Bruker D8 advance X-ray diffractometer with a Cu Kα radiation source. Atomic Force Microscope (AFM) images were obtained by a SPA400HV instrument with an SPI 3800 controller (Seiko Instruments).

The ground state geometries optimization was used by density functional theory (DFT) with PBE0 method and 6-31G (d. p.) basis set[5, 6]. Energies and transition properties were optimized for S_1 using time-dependent density functional theory (TD-DFT) with PBE0 method and 6-31G (d. p.) basis set. All calculation including angles and lengths were performed using Gaussian 09.[7]

Device Fabrication and Characterization

Fabrication and Characterization: OFET devices were fabricated in a bottom-gate top-contact configuration on highly doped n-type Si wafers coated with 300 nm thick thermally grown silicon dioxide. Si wafer was used as the substrate and gate electrode while the silicon dioxide layer served as a dielectric layer. Prior to the modification with octyl trichlorosilane (OTS) according to a reported procedure,[8] the substrates were rinsed by ultrasonication in acetone, deionized water, isopropanol sequentially and were further treated with UV/Ozone for 30 min. Organic semiconductor (OSC) thin films were deposited on the modified substrates by vacuum evaporation. Gold was vacuum-evaporated upon the OSC layers through shadow masks which served as the source and drain electrodes. Width to length ratio (W/L) of source-drain channels defined by the shadow masks was 10 (380/38, 580/58, 780/78, and 980/98 μm, respectively). The performance of OTFT is characterized in the ambient atmosphere using an Agilent B500 semiconductor parameter analyzer. The field-effect mobility and threshold voltages were calculated from the saturation regime according to the following equation:

$$I_d = \frac{W}{2L}\mu C_i(V_g - V_{th})^2$$

where I_d is the source-drain current, C_i is the capacitance per unit area of the gate dielectric layer (SiO_2 modified with OTS), V_g and V_{th} indicate the gate voltage and threshold voltage, respectively.

Stacked multilayer electroluminescence devices were fabricated in this work. Prior to the device fabrication, ITO glasses were cleaned by ultrasonication in acetone, deionized water and isopropanol three times. Organic functional layers and aluminium electrodes were deposited by vacuum evaporation. The emitting area of each pixel defined by shadow masks was 16 mm^2. The device performance was characterized in the ambient atmosphere by Keithley 2400 with BM-7AS luminance colorimeter in F-star Optical Measurement Systems. The electroluminescence spectra and CIE coordinates were obtained by a PR-788 photometer.

Synthesis of 2-(4-Octylphenyl) anthracene (AntPh-C8)

2-bromoanthracene (1.285 g, 5 mmol), 2-(4-octylphenyl)-4, 4, 5, 5-tetramethyl-1, 3, 2-dioxaborolane(2.37 g, 7.5 mmol), 2M potassium carbonate(2.07 g, 15 mmol), toluene and aliquat$_{336}$(several drops) were added into a 300 mL Schleck flask fitted with magnetic bar was added. The mixture solution was degassed with nitrogen for 30 min. After the addition of $Pd(PPh_3)_4$ (0.115 g, 0.1 mmol) in one portion, the reaction mixture was heated up to 105 ℃ and maintained at this temperature for 48 h. After cooling down to room temperature, the reaction mixture was poured into methanol and filtered. The residue was washed with dilute hydrochloric acid, water and methanol sequentially. The crude product was purified by vacuum sublimation. The product was obtained as a yellow solid (1.14 g, 62.2% yield).

^{1}H NMR (300 MHz,$CDCl_3$) δ 8.45 (d, *J* = 9.4 Hz, 2H), 8.19 (s, 1H), 8.07 (d, *J* = 8.9 Hz, 1H), 8.04 – 7.95 (m, 2H), 7.76 (dd, *J* = 8.8, 1.7 Hz, 1H), 7.70 (d, *J* = 8.2 Hz, 2H), 7.54 – 7.42 (m, 2H), 7.33 (d, *J* = 8.2 Hz, 2H), 2.82 – 2.51 (m, 2H), 1.69 (p, *J* = 7.6 Hz, 2H), 1.48 – 1.20 (m, 10H), 0.90 (t, *J* = 6.7 Hz, 3H). ^{13}C NMR (126 MHz, $CDCl_3$) δ 142.54, 138.51, 137.96, 132.26, 132.17, 131.93, 131.03, 129.14, 128.81, 128.38, 128.30, 127.33, 126.59, 126.13, 125.75, 125.59, 125.44, 125.39, 35.84, 32.07, 31.65, 29.67, 29.56, 29.44, 22.84, 14.24.

Synthesis of 2-(4-Octyloxyphenyl) anthracene (AntPh-OC8)

The compound AntPh-OC8 was synthesized from 2-(4-octyloxyphenyl)-4, 4, 5, 5-tetramethyl-1, 3, 2-dioxaborolane and 2-bromoanthracene by Suzuki coupling according to the procedure used for AntPh-C8. AntPh-OC8 was obtained as a pale-yellow solid (1.31 g, 68.7% yield).

^{1}H NMR (300 MHz, $CDCl_3$) δ 8.44 (d, *J* = 7.4 Hz, 2H), 8.14 (s, 1H), 8.06 (d, *J* = 9.0 Hz, 1H), 8.03 – 7.96 (m, 2H), 7.77 – 7.65 (m, 3H), 7.50 – 7.40 (m, 2H), 7.08 – 6.99 (m, 2H), 4.03 (t, *J* = 6.6 Hz, 2H), 1.83 (m, 2H), 1.52 – 1.43 (m, 2H), 1.42 – 1.24 (m, 8H), 0.90 (t, *J* = 6.8 Hz, 3H). ^{13}C NMR (126 MHz, $CDCl_3$) δ 159.16, 137.69, 133.53, 132.30, 132.25, 131.87, 128.81, 128.49, 128.39, 128.28, 126.43, 126.13, 125.68, 125.58, 125.38, 124.82, 115.21, 68.41, 32.00, 29.55, 29.52, 29.42, 26.27, 22.82, 14.23.

Synthesis of 2-Phenylanthracene (AntPh)

The compound AntPh was synthesized from 2-phenyl-4, 4, 5, 5-tetramethyl-1, 3, 2-dioxaborolane

and 2-bromoanthracene by Suzuki coupling according to the procedure used for AntPh-C8. AntPh was obtained as a pale-yellow solid (0.90 g, 71.1% yield).

^{1}H NMR (300 MHz, $CDCl_3$) δ 8.47 (d, J = 10.6 Hz, 2H), 8.24 – 8.18 (m, 1H), 8.09 (d, J = 8.9 Hz, 1H), 8.05 – 7.97 (m, 2H), 7.84 – 7.72 (m, 3H), 7.57 – 7.44 (m, 4H), 7.44 – 7.35 (m, 1H). ^{13}C NMR (75 MHz, $CDCl_3$) δ 141.18, 137.93, 132.20, 132.00, 131.94, 131.00, 129.05, 128.91, 128.37, 128.30, 127.58, 127.51, 126.72, 126.16, 125.81, 125.68, 125.64, 125.54.

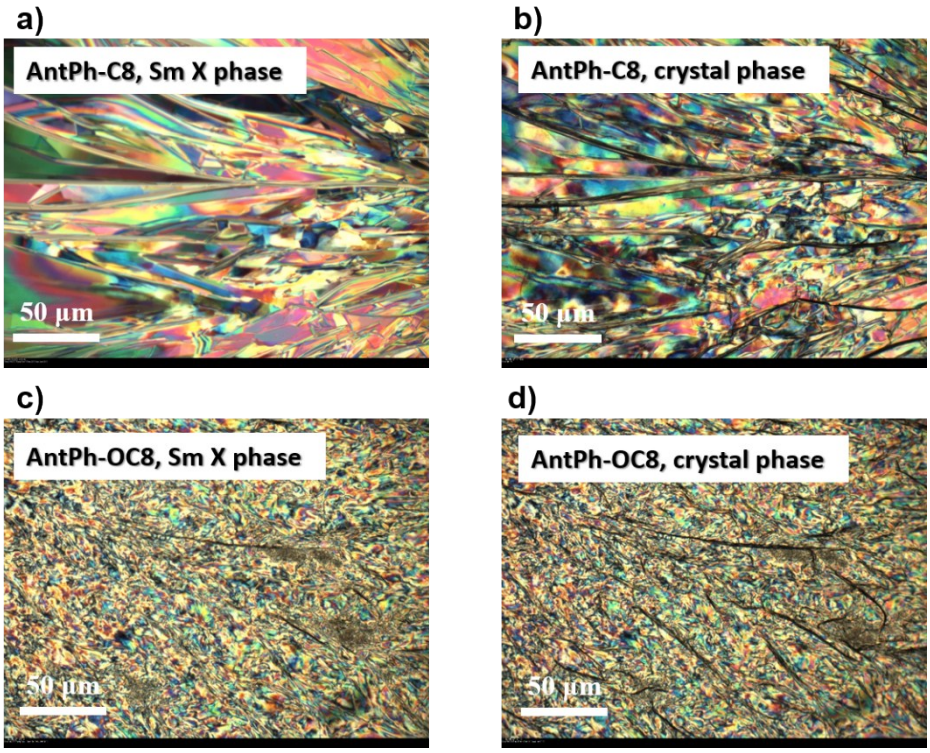

Fig. S1 Polarized optical microscope (POM) images of AntPh-C8 and AntPh-OC8 at various temperatures (a) AntPh-C8 at 140 ℃ (b) AntPh-C8 at 70 ℃ (c) AntPh-OC8 at 140 ℃ (d). AntPh-OC8 at 70 ℃.

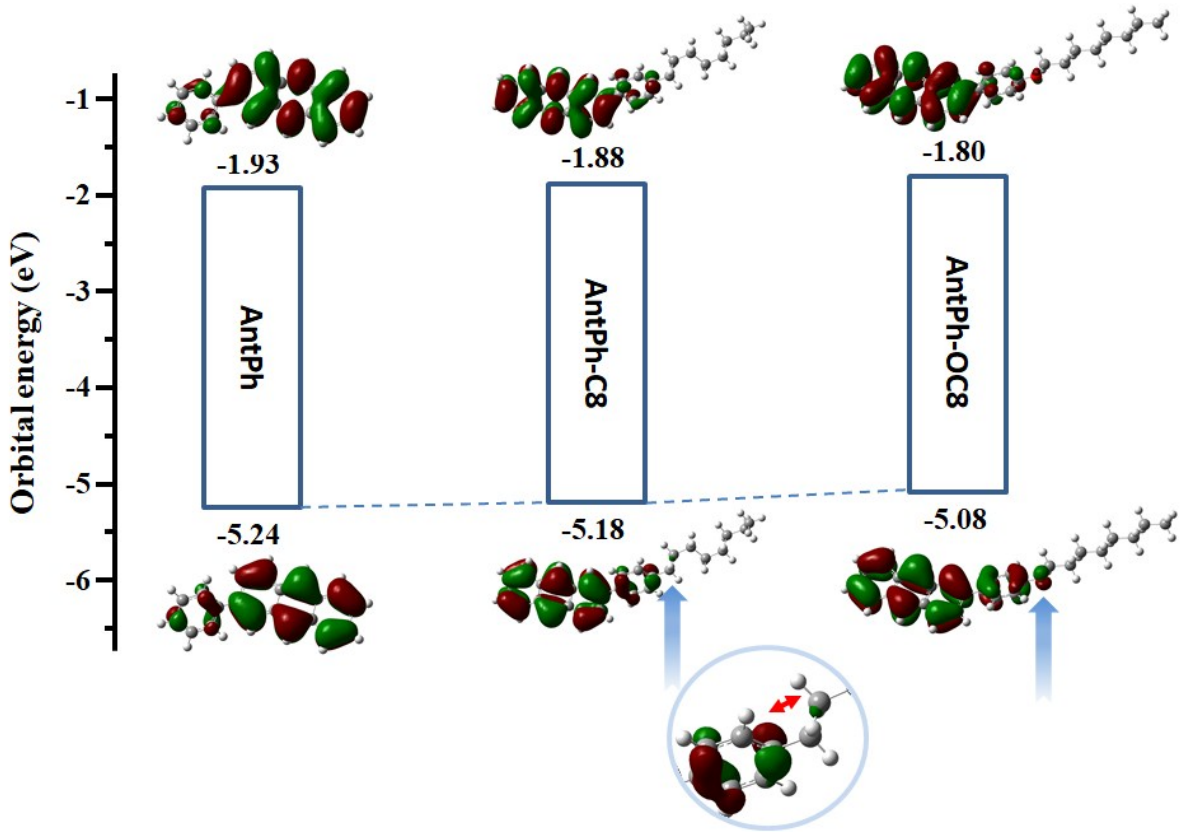

Fig. S2 The molecular orbitals of anthracene derivatives used in this work.

Table S1 Stabilized S1 of AntPh-C8 and AntPh-OC8 compared with AntPh

	S_1 (eV)
AntPh	3.29
AntPh-C8	2.83
AntPh-OC8	2.80

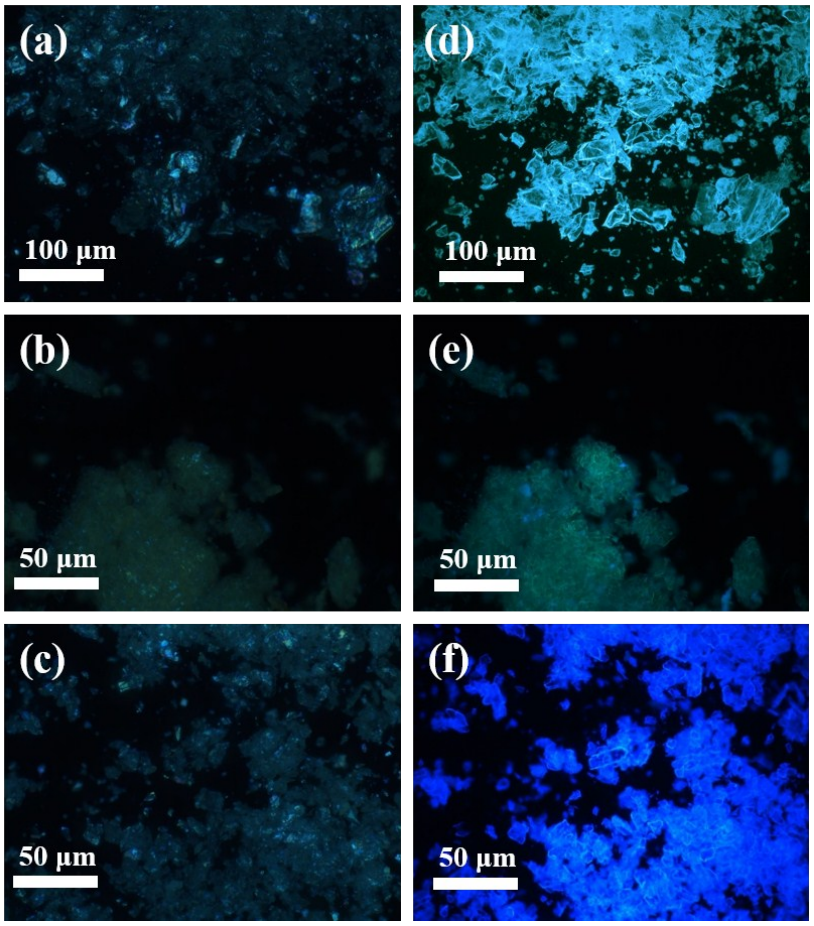

Fig. S3 POM images of AntPh-OC8 (a)(d) , AntPh-C8 (b)(e) and AntPh (c)(f) in powder form under mercury lamp illuminated (d)(e)(f) (fluorescence mode) or halogen lamp illuminated (a)(b)(c) (no fluorescence).

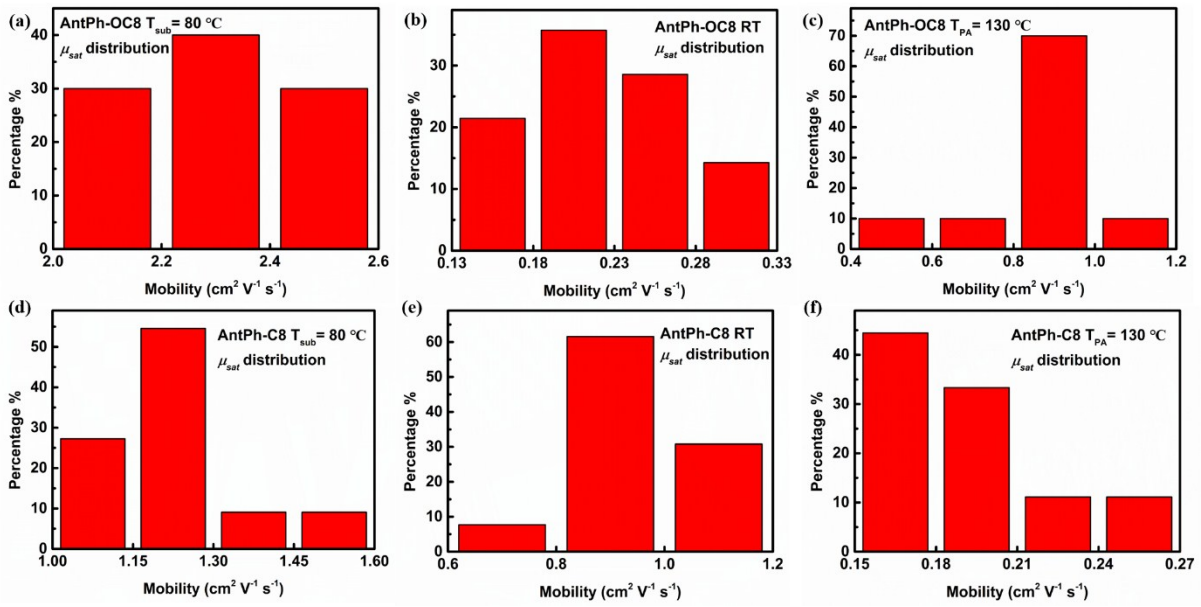

Fig. S4 Saturated mobility distribution of OTFTs based on AntPh-OC8 (a-c) and AntPh-C8 (d-f), which were fabricated at 80 ℃(a) and (d), room temperature (b) and (e) and annealed at 130 ℃ (c) and (f).

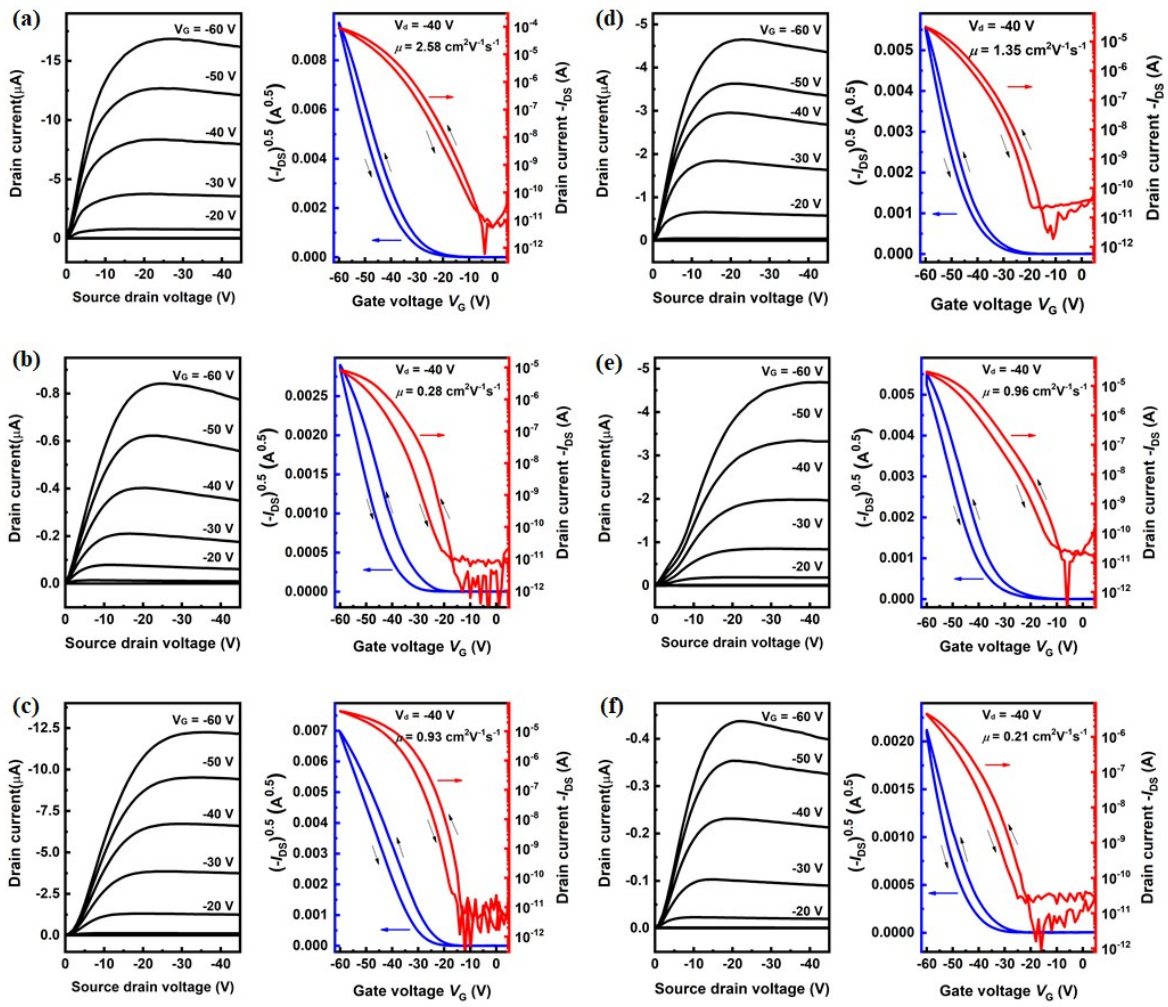

Fig. S5 Representative Id-Vd and Id-Vg characteristics of OTFTs based on AntPh-OC8 (a)(b)(c) and AntPh-C8 (d)(e)(f), which were fabricated at 80 ℃(a)(d), room temperature (b)(e) and annealed at 130 ℃ (c)(f).

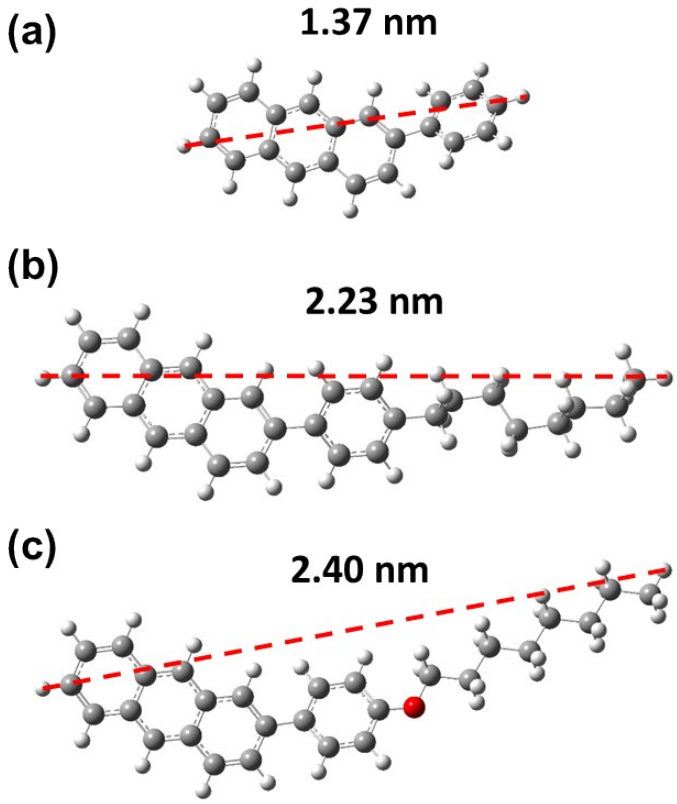

Fig. S6 Molecular length of (a) AntPh (b) AntPh-C8 (c) AntPh-OC8, structures optimized by Gaussian 09.

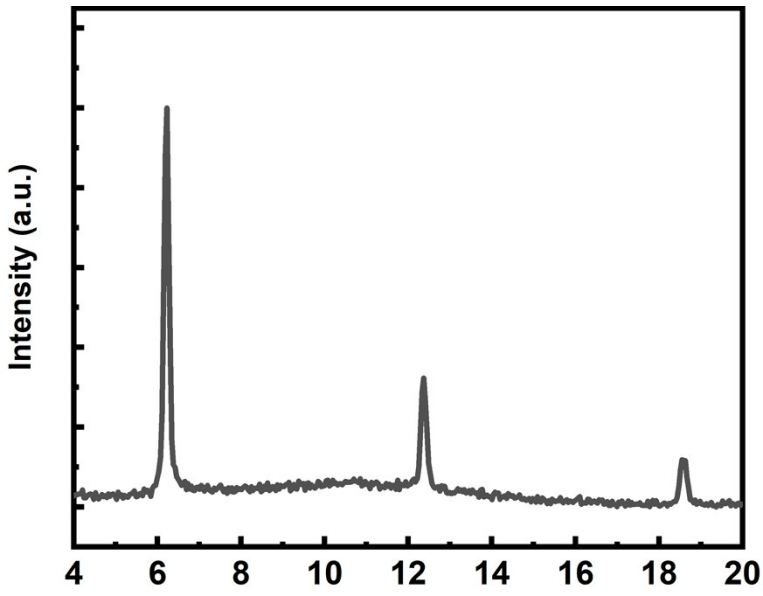

Fig. S7 XRD pattern of the AntPh thin film prepared on the OTS modified SiO2/Si substrates.

NMR Spectra

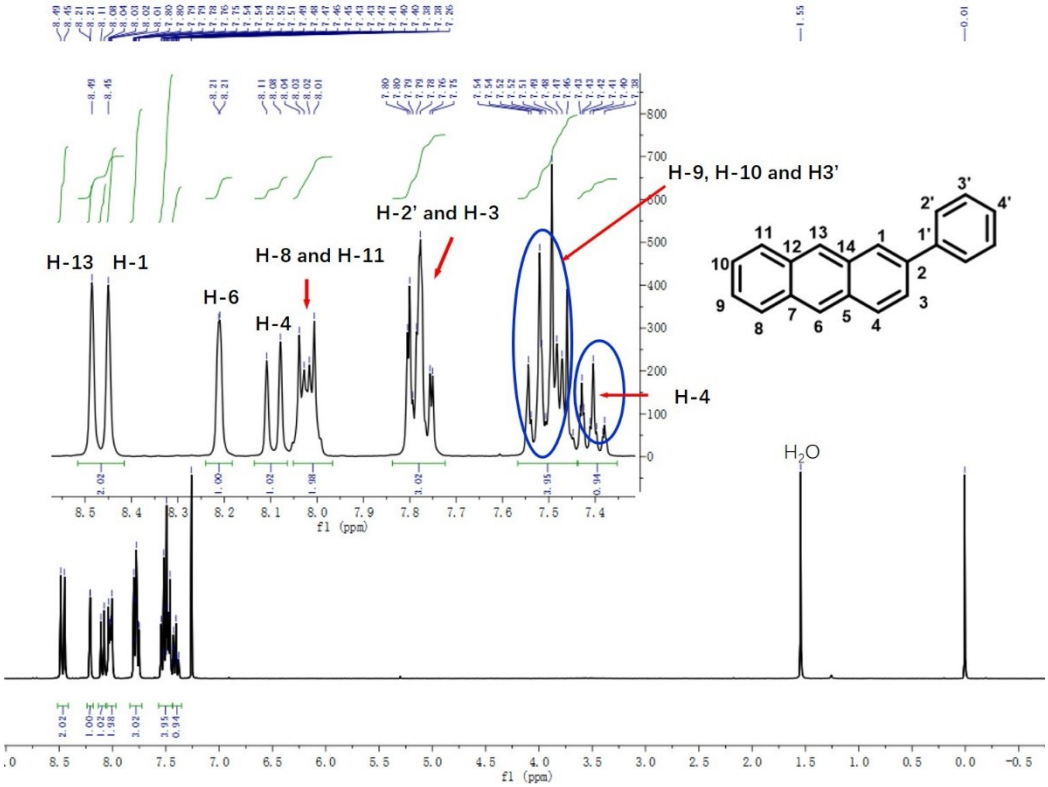

Fig. S8 ^{1}H NMR of AntPh

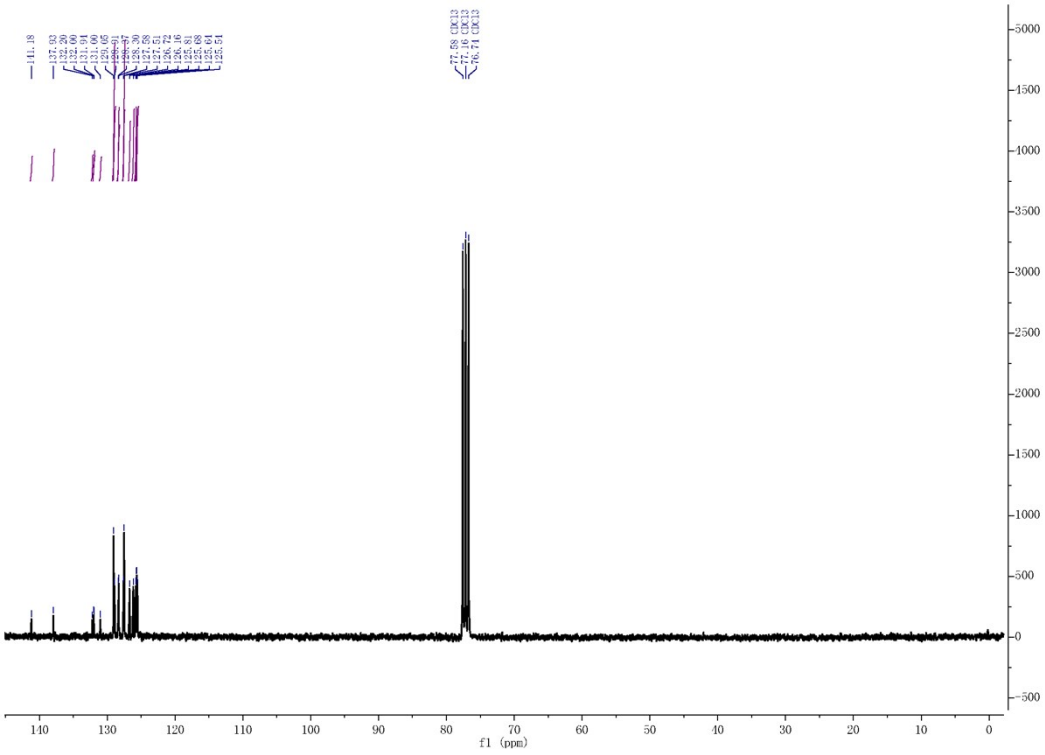

Fig. S9 ^{13}C NMR of AntPh

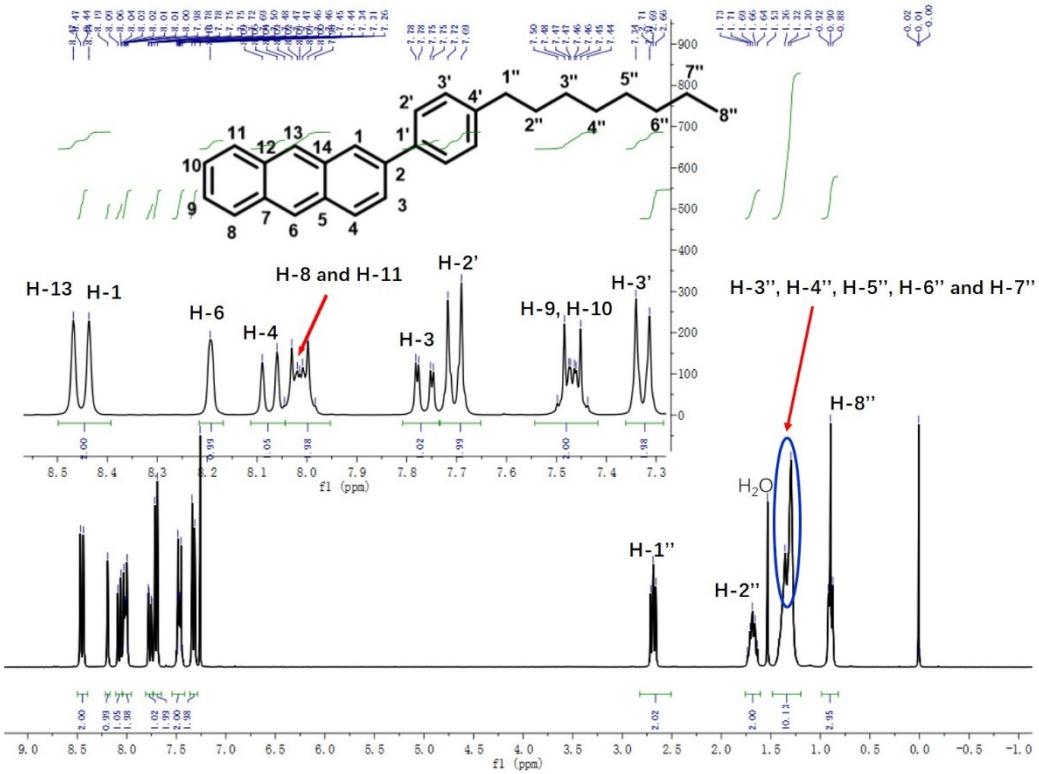

Fig. S10 ^{1}H NMR of AntPh-C8

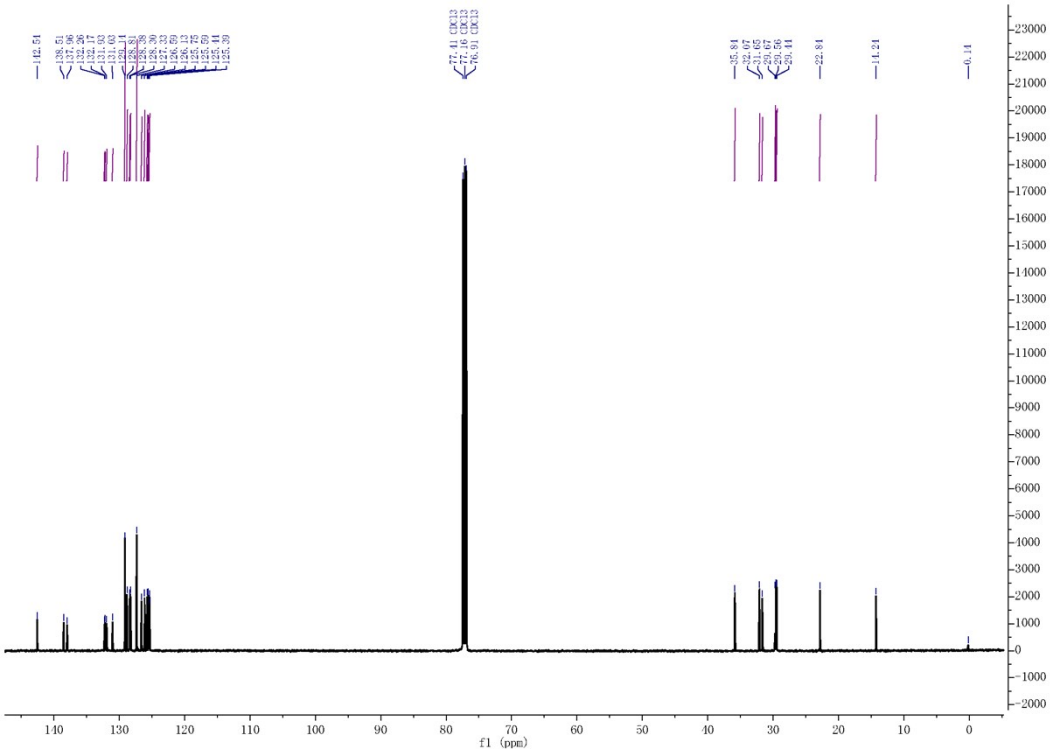

Fig. S11 ^{13}C NMR of AntPh-C8

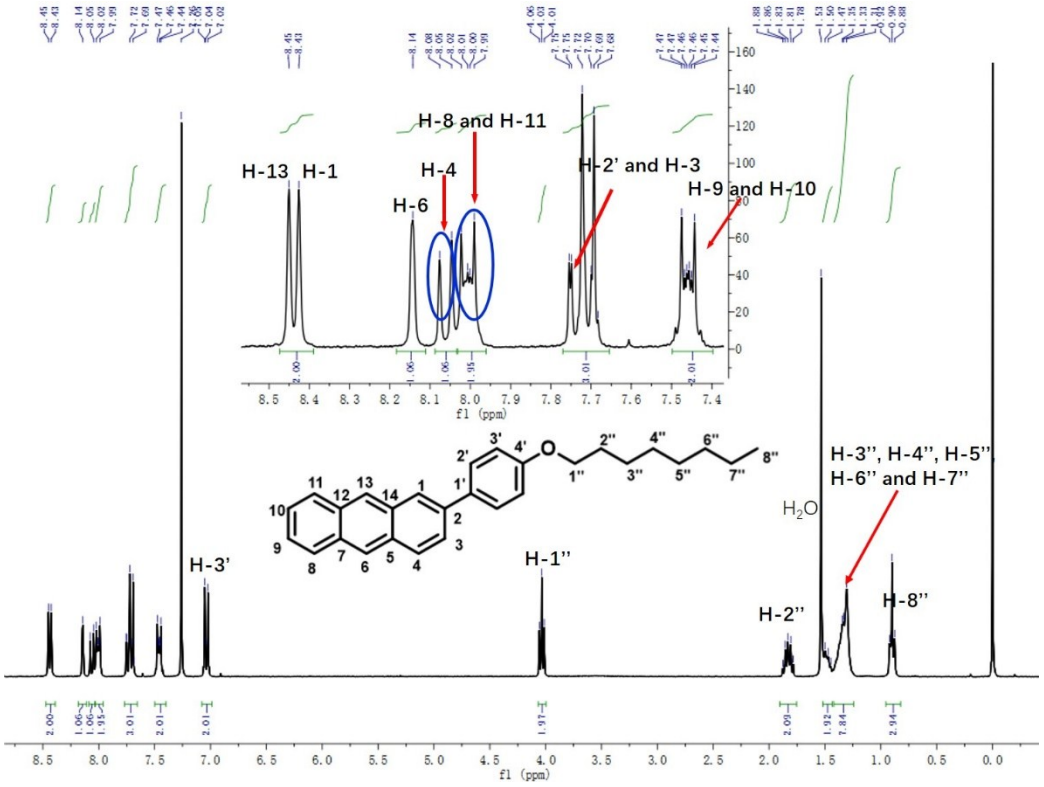

Fig. S12 ^{1}H NMR of AntPh-OC8

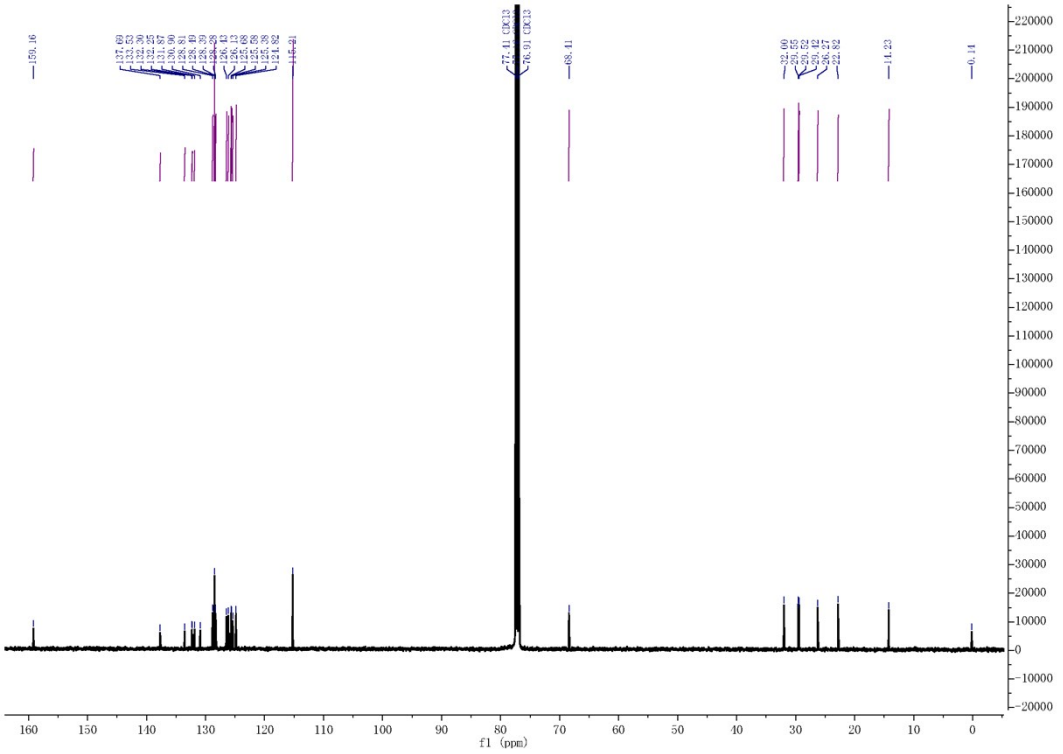

Fig. S13 ^{13}C NMR of AntPh-OC8

References

1. Y. Xu, L. Ren, D. Dang, Y. Zhi, X. Wang and L. Meng, A Strategy of "Self-Isolated Enhanced Emission" to Achieve Highly Emissive Dual-State Emission for Organic Luminescent Materials, *Chem. Eur. J.*, 2018, **24**, 10383-10389.

2. Y. Chen, C. Li, X. Xu, M. Liu, Y. He, I. Murtaza, D. Zhang, C. Yao, Y. Wang and H. Meng, Thermal and Optical Modulation of the Carrier Mobility in OTFTs Based on an Azo-anthracene Liquid Crystal Organic Semiconductor, *ACS. Appl. Mater. Interfaces*, 2017, **9**, 7305-7314.

3. Y. S. Yang, T. Yasuda, H. Kakizoe, H. Mieno, H. Kino, Y. Tateyama and C. Adachi, High performance organic field-effect transistors based on single-crystal microribbons and microsheets of solution-processed dithieno[3,2-b:2',3'-d]thiophene derivatives, *Chem. Commun. (Cambridge, U. K.)*, 2013, **49**, 6483-6485.

4. S. Ito, M. Wehmeier, J. D. Brand, C. Kübel, R. Epsch, J. P. Rabe and K. Müllen, Synthesis and self-assembly of functionalized hexa-peri-hexabenzocoronenes, *Chem. Eur. J.*, 2000, **6**, 4327-4342.

5. K. L. Schuchardt, B. T. Didier, T. Elsethagen, L. Sun, V. Gurumoorthi, J. Chase, J. Li and T. L. Windus, Basis set exchange: a community database for computational sciences, *J. Chem. Inf. Model.*, 2007, **47**, 1045-1052.

6. D. Feller, The role of databases in support of computational chemistry calculations, *J. Comput. Chem.*, 1996, **17**, 1571-1586.

7. M. J. Frisch, G. W. Trucks, H. B. Schlegel, G. E. Scuseria, M. A. Robb, J. R. Cheeseman, G. Scalmani, V. Barone, B. Mennucci, G. A. Petersson, H. Nakatsuji, M. Caricato, X. Li, H. P. Hratchian, A. F. Izmaylov, J. Bloino, G. Zheng, J. L. Sonnenberg, M. Hada, M. Ehara, K. Toyota, R. Fukuda, J. Hasegawa, M. Ishida, T. Nakajima, Y. Honda, O. Kitao, H. Nakai, T. Vreven, J. A. Montgomery Jr, J. E. Peralta, F. Ogliaro, M. Bearpark, J. J. Heyd, E. Brothers, K. N. Kudin, V. N. Staroverov, R. Kobayashi, J. Normand, K. Raghavachari, A. Rendell, J. C. Burant, S. S. Iyengar, J. Tomasi, M. Cossi, N. Rega, N. J. Millam, M. Klene, J. E. Knox, J. B. Cross, V. Bakken, C. Adamo, J. Jaramillo, R. Gomperts, R. E. Stratmann, O. Yazyev, A. J. Austin, R. Cammi, C. Pomelli, J. W. Ochterski, R. L. Martin, K. Morokuma, V. G. Zakrzewski, G. A. Voth, P. Salvador, J. J. Dannenberg, S. Dapprich, A. D. Daniels, O. Farkas, J. B. Foresman, J. V. Ortiz, J. Cioslowski and D. J. Fox, Gaussian 09, Revision B.01, Gaussian, Inc., Wallingford CT, 2010.

8. H. Meng, F. Sun, M. B. Goldfinger, G. D. Jaycox, Z. Li, W. J. Marshall and G. S. Blackman, High-performance, stable organic thin-film field-effect transistors based on bis-5 '-alkylthiophen-2 '-yl-2, 6-anthracene semiconductors, J. Am. Chem. Soc., 2005, 127, 2406-2407.